

# High-quality metamaterial dispersive grating on the facet of an optical fiber

V. Savinov, and N. I. Zheludev

Citation: *Appl. Phys. Lett.* **111**, 091106 (2017); doi: 10.1063/1.4990766

View online: <http://dx.doi.org/10.1063/1.4990766>

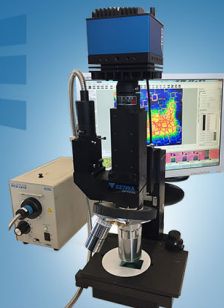
View Table of Contents: <http://aip.scitation.org/toc/apl/111/9>

Published by the [American Institute of Physics](#)

---

---

The logo for SEIWA OPTICAL features the word "SEIWA" in a bold, white, sans-serif font, with "OPTICAL" in a smaller, white, sans-serif font directly below it. To the left of the text is a stylized graphic consisting of three horizontal white bars of varying lengths, creating a triangular shape.



## NEW IR-2200 Microscope

For fast performance and high precision measurements

[LEARN MORE](#) 

## High-quality metamaterial dispersive grating on the facet of an optical fiber

V. Savinov<sup>1,a)</sup> and N. I. Zheludev<sup>1,2</sup>

<sup>1</sup>*Optoelectronics Research Centre and Centre for Photonic Metamaterials, University of Southampton, Southampton SO17 1BJ, United Kingdom*

<sup>2</sup>*Centre for Disruptive Photonic Technologies, TPI, SPMS, Nanyang Technological University, Singapore 637371, Singapore*

(Received 17 June 2017; accepted 15 August 2017; published online 31 August 2017)

Bragg gratings fabricated along the mode propagation direction in optical fibers are a powerful technology for controlling dispersion. Here, we show that a dielectric metamaterial grating with sub-wavelength period fabricated in the thin layer of silicon on the fiber facet exhibits transmission resonance with the quality factor exceeding 300. We demonstrate how focused ion beam patterning, commonly expected to degrade the optical performance of materials, can be exploited to create low-loss photonic nanostructures on the fiber facet. Only a few tens of nanometers in thickness, such facet gratings can be used in compact interconnects, dispersion compensation, and sensing applications. *Published by AIP Publishing.* [<http://dx.doi.org/10.1063/1.4990766>]

Nanoscale metamaterial dispersion element at the fiber tip, reported in this work, provides a viable alternative to key applications of the Fiber Bragg Gratings (FBGs),<sup>1,2</sup> a mainstream and massively deployed technology for dispersion control, spectral filtering, wavelength division multiplexing, as well as channel add-drop functionality, in optical networks and in fiber sensors. The large size of FBGs, which typically lies in the range of centimeters,<sup>2</sup> hampers miniaturization of fiber optic devices. Here, we demonstrate a silicon metamaterial, fabricated on a facet of a silica fiber, which exhibits transmission resonance with the quality factor exceeding 300. Such miniature facet gratings can be used in compact interconnect and dispersion compensation applications in fiber telecoms. We also evaluate the potential for sensor applications.

To achieve a highly dispersive, low-loss response in a thin layer on the fiber tip, we have chosen an all-dielectric metamaterial (see Refs. 3 and 4) design that consists of alternating deep and shallow grooves etched into the silica layer of the fiber, followed by a thin silicon layer on the top (see Fig. 1). The slight difference between the depths and widths of the neighboring grooves provides coupling to the high-quality asymmetric mode supported by this metamaterial. The high-quality mode, which is a type of Fano resonance,<sup>5–8</sup> can be excited by normally incident radiation with electric field polarization perpendicular to the grooves. The mode corresponds to electric displacement field oscillating in anti-phase in the silicon layer of the two grooves, which leads to reduction in the net radiation loss, and thus to establishment of high-quality resonant response. Further discussion on the asymmetric mode supported by the metamaterial will be provided later in the text. Apart from choosing a suitable metamaterial design, achieving high-quality response in a silicon metamaterial depends crucially on depositing and patterning silicon in a way that preserves its low optical loss in the near-infrared region. Here, we use focused ion beam (FIB) milling to structure the end-facet of the optical fiber. This method provides great precision and flexibility; however, it is well-known that direct

FIB-patterning of silicon leads to accumulation of defects.<sup>9–13</sup> For this reason, we pattern silica, i.e., the glass of the fiber, and then deposit silicon over the patterned area, thus preserving its pristine low-loss response.

The fabrication is carried out by stripping a segment of single-mode silica fiber of the protective polymer jacket, leaving a few centimeter long bare silica rod (125  $\mu\text{m}$  in diameter). One end of the fiber is cleaved to create a smooth end-facet, which is coated with a 50 nm thin sacrificial layer of chromium and gold. The tip is then patterned through the sacrificial layer using focused ion beam milling. Following patterning, the metal layer is removed using commercially available wet etchants, leaving a nanostructured silica fiber tip. A layer of amorphous silicon is deposited onto the tip using low pressure chemical vapour deposition. Finally, the bare fiber segment is spliced to a standard FC patch cord (at the non-patterned end). The result is shown in Fig. 1. Compared to other reported methods of fiber nanostructuring,<sup>14–29</sup> this process results in a sample that contains only silica and silicon. Consequently, the metamaterial has very low loss in the near-infrared range and is tolerant both of high optical power as well as heating in general, due to strong adhesion between silica and silicon layers (and high melting point of both materials).

The response of the metamaterial was characterized by illuminating with normally incident linearly polarized white light from an incoherent source and recording the spectrum of light coupled into the optical fiber. The transmission spectra for both parallel (TE) and perpendicular (TM) polarizations (relative to metamaterial grating) are shown in Fig. 2(a). Metamaterial sample exhibits a relatively flat transmission spectrum for both TE and TM polarizations over a broad range of wavelengths, with the exception of a sharp dip at  $\lambda_0 = 1385.5$  nm. This feature appears in both polarizations of incident light, but is significantly sharper for the case of TM polarization. Figure 2(b) compares the measured metamaterial transmission (TM) with the results of full-wave model (also TM). The geometry of the metamaterial used in model, shown in Fig. 3, has been designed based on the cross-section of the experimental sample, shown in the inset of

<sup>a)</sup>v.savinov@orc.soton.ac.uk

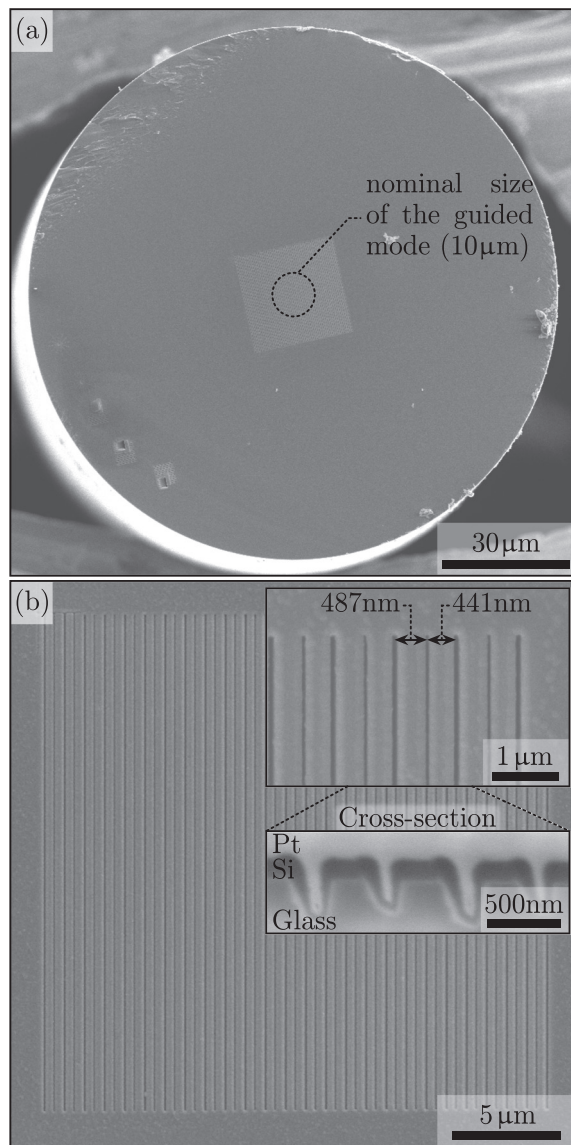


FIG. 1. Low-loss fiber-integrated metamaterial. (a) Electron microscope view of the dielectric metamaterial fabricated on the end-facet of a single-mode optical fiber. The metamaterial is occupying a square patch at the center of the fiber. The dashed circle shows the approximate size of the guided mode. (b) Magnified view of the metamaterial, an array of alternating deep/wide and shallow/narrow grooves. Inset: magnified view of metamaterial's section showing the bottom layer of silica (glass), silicon (Si), and an additional layer of platinum added for contrast (Pt).

Fig. 1(b). For the purposes of modelling, the refractive index of glass was taken as  $n_g = 1.44$ , the wavelength-dependent real part of refractive index of amorphous silicon has been extracted from ellipsometry [e.g.,  $n_{Si}(1400\text{ nm}) = 3.25$ ], while the imaginary part of silicon refractive index has been estimated based on fitting the width of the resonance to experimental observation ( $k_{Si} = 0.015$ ).

Figure 2(b) shows a good agreement between experimentally observed metamaterial transmission and the result of modelling. Simulation reveals that the sharp dip in the metamaterial transmission at  $\lambda_0 = 1385.5\text{ nm}$  corresponds to rise in absorption and is therefore a true metamaterial resonance, i.e., the thin layer of patterned silicon traps light at this wavelength, and retains it long enough to absorb the optical energy despite the low material loss. The distribution

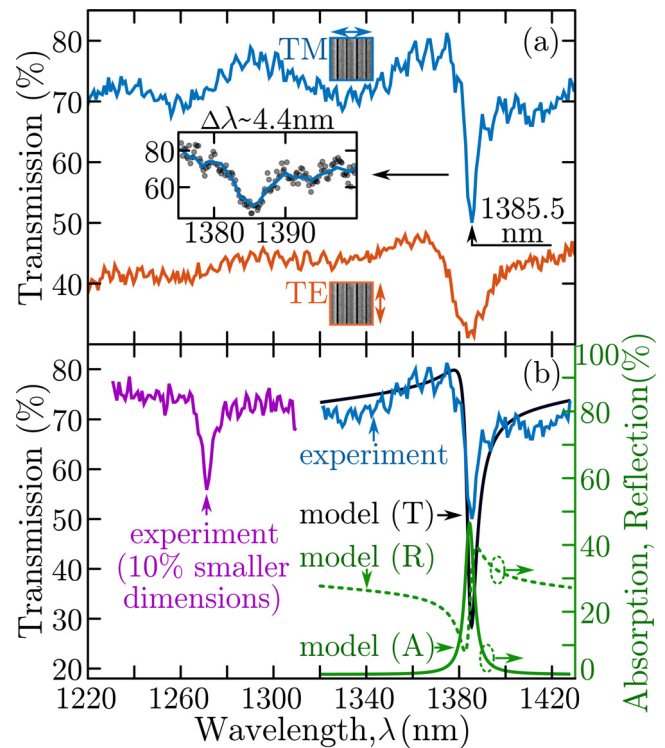


FIG. 2. Optical response of the fiber-integrated metamaterial. (a) Transmission spectra of the metamaterial (shown in Fig. 1) for two polarizations (TE and TM). In both cases, the transmission is normalized with respect to bare fiber transmission. The inset shows the detail of the transmission minimum in TM polarization. The scatter points correspond to measurement with higher spectral resolution. (b) Measured (blue) and modelled (black) transmission of the metamaterial for the case of TM polarization. In both cases the transmission is normalized with respect to bare fiber transmission. The green traces (right axis) show the absorption (solid) and reflection (dashed) of the metamaterial (model). Purple trace corresponds to the transmission of a different metamaterial with the same geometry but 10% reduction in all dimensions.

of electric and magnetic fields in metamaterial at the resonant wavelength (see Fig. 3) shows that this is a type of Fano-resonance,<sup>5</sup> also known as trapped mode resonance, which arises as a result of destructive interference of the transverse-magnetic (TM) modes excited in the two grooves of each unit cell. An alternative equivalent way of understanding the optical response of our metamaterial, is to treat it as a leaky corrugated silica-silicon-air waveguide, which supports guided-mode resonance.<sup>25,30–38</sup> Normally incident light is coupled into the counter-propagating leaky modes supported by the waveguide, which leads to entrapment of light in the metamaterial, manifesting as a sharp dip in transmission.

To further test the reported fabrication technique, another metamaterial was manufactured following the same process, but with all dimensions reduced by approximately 10%. The corresponding transmission spectrum for perpendicular polarization of incident radiation (TM) is shown in Fig. 2(b). As in the case of larger-unit cell metamaterial, the reduced-dimensions metamaterial exhibits a sharp dip in the transmission spectrum at  $\lambda_{0s} = 1271\text{ nm}$ , i.e., 8.2% lower than the original metamaterial sample. This confirms that the dip in metamaterial transmission does arise as a result of patterning and can be tuned to a wavelength of choice by appropriate adjustments to metamaterial geometry.

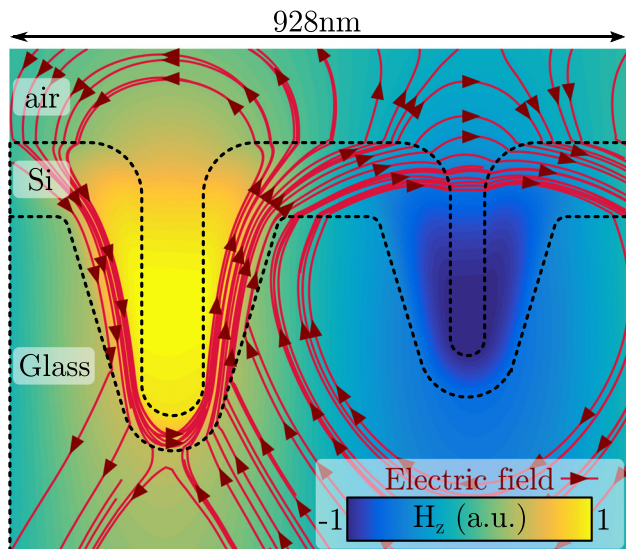


FIG. 3. Modelled metamaterial response at  $\lambda_0 = 1385$  nm. The magnetic (colormap) and electric (red field-lines) field distribution at the metamaterial (unit cell) when it is driven by normally incident radiation polarized perpendicular to the metamaterial grooves (TM). In the case of magnetic field, the colormap denotes the field component that points out of the page ( $H_z$ ). The black contour lines denote the metamaterial geometry, which consists out of a layer of silicon (Si) on top of silica (glass).

The quality factors of metamaterial transmission minima ( $Q = \lambda_0/\Delta\lambda$ ) are  $Q \sim 310$  and  $Q \sim 270$ , for the original metamaterial and the reduced-dimensions metamaterial, respectively. We note that quality factors reached in our metamaterials are of the same order as in the best planar dielectric metamaterials.<sup>4,39–41</sup> In principle, one can develop further optimizations, such as annealing to convert amorphous silicon into poly-crystalline silicon and to reduce the surface roughness, but the improvements are likely to be modest even if the performance of optimized fiber-tip metamaterials would reach that of the state-of-the-art planar all-dielectric metamaterials ( $Q \sim 500$ – $600$ ).

The narrow resonance exhibited by the fiber-tip metamaterial suggests highly dispersive response that could be used to compensate dispersion<sup>38,42,43</sup> of short segments of telecom fibers, for example, in miniaturized fiber-optic devices. The group delay dispersion of the metamaterial, extracted from the full-wave model (see Figs. 2 and 3), is shown in Fig. 4. As one would expect, the transmission minimum of the metamaterial corresponds to maximum dispersion; however, dispersion remains large even in the spectral range of high transmission. The dashed line in Fig. 4 indicates the minimum level of positive dispersion necessary to compensate the (negative) dispersion of 1 m of standard optical fiber. It follows that metamaterial response is sufficiently dispersive (at  $\lambda \sim 1380$  nm) to provide dispersion compensation even at near-maximum transmission level of  $\sim 80\%$ .

An alternative application for high-quality response of the fiber-tip metamaterial is ambient refractive index sensing. Indeed, according to simulations, our metamaterial can deliver sensitivity of  $\sim 400$  nm/RIU (see the [supplementary material](#)), which is comparable to the state-of-the-art fiber based refractive index sensors.<sup>14,16–18,20,22,23,26,27,44–47</sup> Importantly, in our case, the large sensitivity of metamaterial to ambient refractive index is accompanied by very narrow

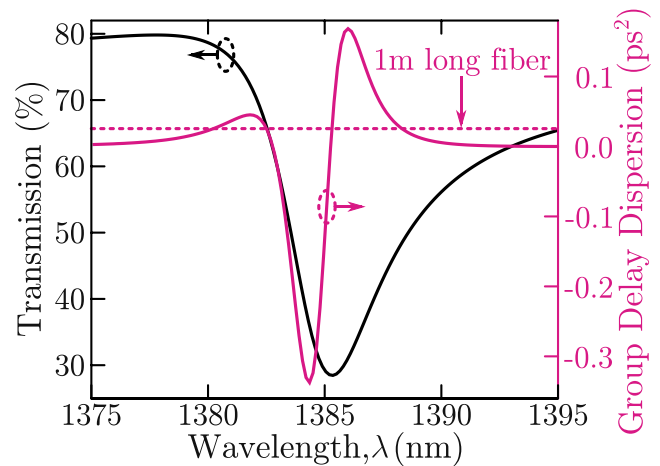


FIG. 4. Group delay dispersion of the fiber-tip metamaterial (model; see Fig. 3). Black trace (left axis) shows the metamaterial transmission (relative to bare fiber). Pink trace (right axis) shows the group delay dispersion of the metamaterial. The dashed line denotes the level of dispersion necessary to compensate (negative) dispersion of a 1 m long telecom fiber (assuming fiber group velocity dispersion is  $\sim 20$  ps/nm km).

line-width of the resonant dip ( $\Delta\lambda \sim 5$  nm), leading to a high figure of merit (sensitivity/ $\Delta\lambda$ )  $\sim 20$ /RIU.

In conclusion, we have developed low loss dielectric metamaterials, with narrow transmission resonances and strongly dispersive response, on tips of silica fibers. We have demonstrated resonance quality factors in excess of 300 and corresponding group delay dispersion over  $0.3$  ps<sup>2</sup>. Our results suggest that fiber-tip metamaterials could find applications in compact fiber-optic devices.

See [supplementary material](#) for simulations evaluating performance of the metamaterial as refractometric sensor.

The authors acknowledge financial support from UK Engineering and Physical Sciences Research Council (Grant No. EP/M009122/1) and the Singapore Ministry of Education (Grant No. MOE2011-T3-1-005). The data from this paper can be obtained from the University of Southampton ePrints research repository: <https://doi.org/10.5258/SOTON/D0191>.

<sup>1</sup>R. Kashyap, *Fiber Bragg Gratings* (Academic Press, 1999).

<sup>2</sup>G. P. Agrawal, *Fiber-Optic Communication Systems*, 4th ed. (Wiley, 2010).

<sup>3</sup>A. M. Urbas, Z. Jacob, L. Dal Negro, N. Engheta, A. D. Boardman, P. Egan, A. B. Khanikaev, V. Menon, M. Ferrera, N. Kinsey *et al.*, “Roadmap on optical metamaterials,” *J. Opt.* **18**, 093005 (2016).

<sup>4</sup>S. Jahani and Z. Jacob, “All dielectric metamaterials,” *Nat. Nanotechnol.* **11**, 23 (2016).

<sup>5</sup>B. Luk’yanchuk, N. I. Zheludev, S. A. Maier, N. J. Halas, P. Nordlander, H. Giessen, and C. T. Chong, “The Fano resonance in plasmonic nanostructures and metamaterials,” *Nat. Mater.* **9**, 707 (2010).

<sup>6</sup>J. Zhang, K. F. MacDonald, and N. I. Zheludev, “Near-infrared trapped mode magnetic resonance in an all-dielectric metamaterial,” *Opt. Express* **21**, 26721 (2013).

<sup>7</sup>J. Zhang, K. F. MacDonald, and N. I. Zheludev, “Nonlinear dielectric optomechanical metamaterials,” *Light: Sci. Appl.* **2**, e96 (2013).

<sup>8</sup>A. Karvounis, J.-Y. Ou, W. Wu, K. F. MacDonald, and N. I. Zheludev, “Nano-optomechanical nonlinear dielectric metamaterials,” *Appl. Phys. Lett.* **107**, 191110 (2015).

<sup>9</sup>L. A. Giannuzzi and F. A. Stevie, “A review of focused ion beam milling techniques for TEM specimen preparation,” *Micron* **30**, 197 (1999).

- <sup>10</sup>N. I. Kato, "Reducing focused ion beam damage to transmission electron microscopy samples," *J. Electron. Microsc.* **53**, 451 (2004).
- <sup>11</sup>J. P. McCaffrey, M. W. Phaneuf, and L. D. Madsen, "Surface damage formation during ion-beam thinning of samples for transmission electron microscopy," *Ultramicroscopy* **87**, 97 (2001).
- <sup>12</sup>S. Reyntjens and R. Pueres, "A review of focused ion beam applications in microsystem technology," *J. Micromech. Microeng.* **11**, 287 (2001).
- <sup>13</sup>S. Rubanov and P. R. Munroe, "FIB-induced damage in silicon," *Microscopy* **214**, 213 (2004).
- <sup>14</sup>G. Kostovski, P. R. Stoddart, and A. Mitchell, "The optical fiber tip: An inherently light-coupled microscopic platform for micro- and nanotechnologies," *Adv. Mater.* **26**, 3798 (2014).
- <sup>15</sup>A. Khan, S. Li, X. Tang, and W.-D. Li, "Nanostructure transfer using cyclic olefin copolymer templates fabricated by thermal nanoimprint lithography," *J. Vac. Sci. Technol. B* **32**, 06F102 (2014).
- <sup>16</sup>M. Pisco, F. Galeotti, G. Quero, A. Iadicco, M. Giordano, and A. Cusano, "Miniaturized sensing probes based on metallic dielectric crystals self-assembled on optical fiber tips," *ACS Photonics* **1**, 917 (2014).
- <sup>17</sup>Z. Zhang, Y. Chen, H. Liu, H. Bae, D. A. Olson, A. K. Gupta, and M. Yu, "On-fiber plasmonic interferometer for multiparameter sensing," *Opt. Express* **23**, 10732 (2015).
- <sup>18</sup>M. Boerkamp, Y. Lu, J. Mink, Z. Zobenica, and R. W. van der Heijden, "Multiple modes of a photonic crystal cavity on a fiber tip for multiple parameter sensing," *J. Lightwave Technol.* **33**, 3901 (2015).
- <sup>19</sup>A. Micco, A. Ricciardi, M. Pisco, V. La Ferrara, and A. Cusano, "Optical fiber tip templating using direct focused ion beam milling," *Sci. Rep.* **5**, 15935 (2015).
- <sup>20</sup>Y. Liu, Z. Huang, F. Zhou, X. Lei, B. Yao, G. Mengb, and Q. Mao, "Highly sensitive fibre surface-enhanced Raman scattering probes fabricated using laser-induced self-assembly in a meniscus," *Nanoscale* **8**, 10607 (2016).
- <sup>21</sup>J. Zhang, S. Chen, T. Gong, X. Zhang, and Y. Zhu, "Tapered fiber probe modified by Ag nanoparticles for SERS detection," *Plasmonics* **11**, 743 (2016).
- <sup>22</sup>X. He, H. Yi, J. Long, X. Zhou, J. Yang, and T. Yang, "Plasmonic crystal cavity on single-mode optical fiber end facet for label-free biosensing," *Appl. Phys. Lett.* **108**, 231105 (2016).
- <sup>23</sup>P. Jia, Z. Yang, J. Yang, and H. Ebdorff-Heidepriem, "Quasiperiodic nanohole arrays on optical fibers as plasmonic sensors: Fabrication and sensitivity determination," *ACS Sens.* **1**, 1078 (2016).
- <sup>24</sup>G. Calafiore, A. Koshelev, F. I. Allen, S. Dhuey, S. Sassolini, E. Wong, P. Lum, K. Munechika, and S. Cabrini, "Nanoimprint of a 3D structure on an optical fiber for light wavefront manipulation," *Nanotechnology* **27**, 375301 (2016).
- <sup>25</sup>D. Wawro, S. Tibuleac, R. Magnusson, and H. Liu, "Optical fiber endface biosensor based on resonances in dielectric waveguide gratings," *Proc. SPIE* **3911**, 86 (2000).
- <sup>26</sup>D. C. Abeysinghe, S. Dasgupta, J. T. Boyd, and H. E. Jackson, "A novel MEMS pressure sensor fabricated on an optical fiber," *IEEE Photonics Technol. Lett.* **13**, 993 (2001).
- <sup>27</sup>S. Feng, S. Darmawi, T. Henning, P. J. Klar, and X. Zhang, "A miniaturized sensor consisting of concentric metallic nanorings on the end facet of an optical fiber," *Small* **8**, 1937 (2012).
- <sup>28</sup>V. M. Sundaram and S.-B. Wen, "Fabrication of micro-optical devices at the end of a multimode optical fiber with negative tone lift-off EBL," *J. Micromech. Microeng.* **22**, 125016 (2012).
- <sup>29</sup>C. Liberale, P. Minzioni, F. Bragheri, F. De Angelis, E. Di Fabrizio, and I. Cristiani, "Miniaturized all-fibre probe for three-dimensional optical trapping and manipulation," *Nat. Photonics* **1**, 723 (2007).
- <sup>30</sup>R. Magnusson and S. S. Wang, "New principle for optical filters," *Appl. Phys. Lett.* **61**, 1022 (1992).
- <sup>31</sup>S. S. Wang and R. Magnusson, "Theory and applications of guided-mode resonance filters," *Appl. Opt.* **32**, 2606 (1993).
- <sup>32</sup>R. Magnusson, S. S. Wang, T. D. Black, and A. Sohn, "Resonance properties of dielectric waveguide gratings: Theory and experiments at 4-18 GHz," *IEEE Trans. Antennas Propag.* **42**, 567 (1994).
- <sup>33</sup>S. Peng and G. M. Morris, "Experimental demonstration of resonant anomalies in diffraction from two-dimensional gratings," *Opt. Lett.* **21**, 549 (1996).
- <sup>34</sup>D. Rosenblatt, A. Sharon, and A. A. Friesem, "Resonant grating waveguide structures," *IEEE J. Quantum Electron.* **33**, 2038 (1997).
- <sup>35</sup>D. Shin, S. Tibuleac, T. A. Maldonado, and R. Magnusson, "Thin-film optical filters with diffractive elements and waveguides," *Opt. Eng.* **37**, 2634 (1998).
- <sup>36</sup>H. Kikuta, H. Toyota, and W. Yu, "Optical elements with subwavelength structured surfaces," *Opt. Rev.* **10**, 63 (2003).
- <sup>37</sup>R. Magnusson, Y. Ding, K. J. Lee, D. Shin, P. Priambodo, P. P. Young, and T. A. Maldonado, "Photonic devices enabled by waveguide-mode resonance effects in periodically modulated films," *Proc. SPIE* **5225**, 20 (2003).
- <sup>38</sup>R. Magnusson, M. Shokoooh-Saremi, and X. Wang, "Dispersion engineering with leaky-mode resonant photonic lattices," *Opt. Express* **18**, 108 (2010).
- <sup>39</sup>S. Campione, S. Liu, L. I. Basilio, L. K. Warne, W. L. Langston, T. S. Luk, J. R. Wendt, J. L. Reno, G. A. Keeler, I. Brener, and M. B. Sinclair, "Broken symmetry dielectric resonators for high quality factor Fano metasurfaces," *ACS Photonics* **3**, 2362 (2016).
- <sup>40</sup>Y. Yang, I. I. Kravchenko, D. P. Briggs, and J. Valentine, "All-dielectric metasurface analogue of electromagnetically induced transparency," *Nat. Commun.* **5**, 5753 (2014).
- <sup>41</sup>Y. Yang, W. Wang, A. Boulesbaa, I. I. Kravchenko, D. P. Briggs, A. Poretzky, D. Geohagan, and J. Valentine, "Nonlinear Fano-resonant dielectric metasurfaces," *Nano Lett.* **15**(11), 7388 (2015).
- <sup>42</sup>F. Schreier, M. Schmitz, and O. Bryngdahl, "Pulse delay at diffractive structures under resonance conditions," *Opt. Lett.* **23**, 1337 (1998).
- <sup>43</sup>B. Dastmalchi, P. Tassin, T. Koschny, and C. M. Soukoulis, "Strong group-velocity dispersion compensation with phase-engineered sheet metamaterials," *Phys. Rev. B* **89**, 115123 (2014).
- <sup>44</sup>A. Dhawan, J. F. Muth, D. N. Leonard, M. D. Gerhold, J. Gleeson, T. Vo-Dinh, and P. E. Russell, "Focused ion beam fabrication of metallic nanostructures on end faces of optical fibers for chemical sensing applications," *J. Vac. Sci. Technol. B* **26**, 2168 (2008).
- <sup>45</sup>Y. Lin, Y. Zou, Y. Mo, J. Guo, and R. G. Lindquist, "E-beam patterned gold nanodot arrays on optical fiber tips for localized surface plasmon resonance biochemical sensing," *Sensors* **10**, 9397 (2010).
- <sup>46</sup>A. Ricciardi, M. Consales, G. Quero, A. Crescitelli, E. Esposito, and A. Cusano, "Lab-on-Fiber devices as an all around platform for sensing," *Opt. Fiber Technol.* **19**, 772 (2013).
- <sup>47</sup>P. Jia and J. Yang, "Integration of large-area metallic nanohole arrays with multimode optical fibers for surface plasmon resonance sensing," *Appl. Phys. Lett.* **102**, 243107 (2013).